Uptake and transformation of oxybenzone in the presence of TiO_2: impact of nanoparticles on the plant remediation of an organic UV filter

Feiran Chen[#], Peter Schröder*

Research Unit Comparative Microbiome Analysis, Helmholtz Zentrum München, GmbH, German Research Center for Environmental Health, Ingolstädter Landstraße 1, D-85764 Neuherberg, Germany, email: peter.schroeder@helmholtz-muenchen.de (P. Schröder)
[#]*Present address: Institute of Environmental Processes and Pollution Control, School of Environmental and Civil Engineering, Jiangnan University, Wuxi 214122, China*

ABSTRACT

Oxybenzone (OBZ) present in the environment as an emerging contaminant may occur jointly with the nanoparticle TiO_2 due to the typical composition of many sunscreens. Thus, potential effects caused by TiO_2 must be considered when investigating the environmental fate of sunscreens and also when plant performance with regard to remediation of OBZ is scrutinized. Toxicity effects of OBZ and TiO_2 on plant development were evaluated by recording germination rates and root lengths of tomato and barley. Results showed that OBZ significantly inhibited germination rate of tomato seeds, while no effect was observed for germination of barley seeds. Interestingly, co-exposure with TiO_2 lowered the toxicity of OBZ on the tomato seedlings as there were no differences on germination rate and root length between co-exposure and control treatments. Moreover, growth inhibition tests with *Lemna minor* showed that addition of TiO_2 even enhanced plant growth by increasing the frond area. Furthermore, influence of TiO_2 (3 mg/L) on removal of OBZ (5 μM) by plants was examined with respect to the variations in uptake and metabolism of OBZ in a hairy root culture system. Co-exposure to TiO_2 amplified the accumulation of OBZ in plants, while transient slower transformation to OBZ metabolites was recognized when TiO_2 had been added. Therefore, it can be concluded that Ti nanoparticles may generally reduce the phytotoxicity of OBZ and increase the uptake of this compound in phytoremediation, while the interaction with the transformation capacity should be considered when applying phytoremediation for UV-filter contaminated water.

Keywords: Oxybenzone; TiO_2; Uptake; Transformation; Hairy roots

1. Introduction

UV filters are common components among the personal care products (PCPs), and they have been suspected to become emerging contaminants due to their massive release during recreational activities in fresh and seawater as well as from effluents of wastewater treatment plants fed with municipal wastewater [1]. Commercial sunscreens may contain both chemical (organic, absorb UV radiation) and physical (inorganic, reflect UV) filters [2]. Oxybenzone (OBZ) is a typical organic ingredient added in the sun protective products. Over 81% of the 231 PCPs collected from United States and China contain this compound [3]. The widespread use of OBZ has led to its release into the environment and today it is one of the most frequently detected UV filters in surface water and wastewater [1,4–7]. Across the world, highest concentrations up to 1.395 mg/L of OBZ have been detected along Trunk Bay in Virgin Islands [8]. Accumulation of OBZ has also been reported in organisms involved in the aquatic food chain [1,7] and the compound has been proved in vivo as an endocrine-active agent to fish [9]. Moreover, the presence of OBZ has been associated with the deterioration of coral reefs [10]. Titanium dioxide (TiO_2), a well-known nanomaterial, is widely incorporated as an inorganic UV filter

* Corresponding author.

in cosmetics and industrial products, but it is also applied extensively to photocatalyse breakdown of environmental pollutants [2]. The US annual production of nano-TiO_2 is estimated to reach 2.5 million metric tons in 2025 [11]. Both, the growth of production and application inevitably enhance the entry of TiO_2 into the environment. Recently 3,000 μg/L of titanium has been detected in raw sewage water [12], which ultimately could lead to interactions with the environment and living organisms.

Phytoremediation has been recommended as a suitable technology to cope with emerging contaminants in many compartments of the aquatic environment. Previous studies focused primarily on the single treatment of OBZ by aquatic higher plants [13], however, since commercial sun protective products normally contain several components, including nanoparticles, in this study, OBZ and TiO_2 were chosen as the compounds of interest, which are often combined to provide strong photoprotection.

Nanoparticles have been demonstrated to be beneficial for the delivery of biomolecules into plant cells [14], and at the same time they have been reported to alter the bioavailability and fate of other contaminants. The accumulation of the pesticide chlordane in crops increased 34.9% when exposed to C_{60} fullerenes [15]. Zhang et al. [16] demonstrated the enhanced bioaccumulation of cadmium in carp in the presence of TiO_2. Also, the nutrient uptake patterns in *Elodea canadensis* were altered with the addition of TiO_2, and concentrations of all the elements showed significant correlations with each other [17].

Considering the influence of nanoparticles on many organic chemicals, it is essential to investigate the treatment efficiency of OBZ by plant with respect to the nano-TiO_2. This study aimed to scrutinize the above aspects. Therefore, the toxicities of OBZ and TiO_2 on plants were estimated by evaluating germination rate and root length of barley and tomato seedlings. In addition, growth inhibition was tested with *Lemna minor* growing hydroponically in microplates, and the resulting impact on frond area and photosynthetic pigments was determined. More importantly, a well-established horseradish (*Armoracia rusticana*) hairy root system (HRs) was selected for the current study, with the advantages of fast growth, free of bacterial interference. Since the results obtained from HRs have been proven to be reliable and can be extended to intact plants, this system represents an appropriate approach for characterizing the fundamental processes in plants. The influence of TiO_2 on uptake and transformation of OBZ was therefore studied in HRs with and without addition of TiO_2 in aqueous suspensions. Furthermore, enzyme activities were assayed to evaluate the effects of both compounds on the performance of the plant detoxification system and consequences for water and food quality.

2. Materials and methods

2.1. Seed germination tests

Seeds of barley (*Hordeum vulgare*) and tomato (*Lycopersicon esculentum*) were placed on wet filter paper and germinated in suspensions containing either 5 μM OBZ or 3 mg/L TiO_2 alone, or 5 μM OBZ mixed with 3 mg/L TiO_2, respectively. Seeds free of both compounds were regarded as control. TiO_2 was suspended in ultrapure water (MilliQ, Millipore

Corporation, USA), the suspension was sonicated twice for 2 min, using a ultrasonic homogenizer (SonoPlus HD 2070, Bandelin, Germany) at an energy of 40 W [18]. Prior to use, the suspension was filtered through membrane filter of 220 nm (PVDF (polyvinylidene fluoride), Carl Roth GmbH, Germany) to eliminate large agglomerates [19]. Two plates were prepared for each treatment, in every plate 15 seeds with same shape were arranged with same space. All seeds were incubated at room temperature, barley seeds were placed in dark for 3 d and tomato seeds were exposed with a 15/9 h light/dark cycle for 10 d in a growth chamber at the Helmholtz Center in Munich, Germany. The number of germinated seeds was counted and the root length was recorded by an image processing software (ImageJ).

2.2. Microbiotest with L. minor

A microbiotest was designed according to the commercial protocol with modifications [20]. In short, *L. minor* plantlets with homogeneous frond size were selected and transferred to 96-well microplate containing Steinberg medium [21]. Each well contained one frond, 24 wells were integrated for each treatment. Treatments including OBZ/TiO_2 alone or in mixture were set up similar to those in the seed germination tests. Media in control wells were without xenobiotic pollution. The plate was incubated for 3 d at 25°C in the laboratory. Digital photos were taken at both beginning and end of the incubation, and the frond area at these two time points was calculated with the help of ImageJ. The growth of *Lemna* fronds was evaluated by the relative growth rate, which is calculated on the basis of changes in frond area determined during the course of the 3-d exposure period. Additionally, chlorophyll and carotenoid contents of corresponding fronds after 7 d incubation were determined as described previously [22], briefly, 0.05 g freshly ground frond powder was immersed with 0.6 mL cold 95% ethanol, after 1 h storage in a dark fridge (4°C) the samples were centrifuged at 4,000g for 1 min, the resulting supernatant was collected while the pellet was dissolved in 95% ethanol, stored and centrifuged again, the same procedure was repeated twice until the fronds were virtually pale. Supernatants from each centrifugation were collected and combined; the samples were measured spectrophotometrically at 664.1, 648.1 and 470 nm according to the method of Lichtenthaler and Buschmann [23]. The pigment contents were expressed as μg/g fresh weight.

2.3. Hairy root culture experiment

Hairy root culture of horseradish had been obtained formerly by transformation of nodal segments by *Agrobacterium rhizogenes* strain A4 [24]. After subdivision, roots obtained from the same generation were adopted and grown in 250 mL Erlenmeyer flask with 100 mL Murashige and Skoog medium with addition of sucrose inositol and thiamine for 10 d. The experiment was initiated by incubating the roots in medium containing 5 μM OBZ supplemented in the presence or absence of 3 mg/L TiO_2, roots added independently with 3 mg/L TiO_2, control roots free of both compounds and medium without roots were set up under the same conditions. Triplicate samples of roots and medium from each treatments (including control) were harvested

at 0, 2, 4 and 7 d, respectively. Root samples were frozen in liquid nitrogen and stored at −80°C. All the chemicals used were of analytical grade.

2.4. Extraction of roots

OBZ and its metabolites were extracted according to the method described previously [25]. In short, 0.5 g of plant material were ground and extracted with 1.5 mL H$_2$O/acetonitrile (30/70, v/v). After 5 min ultrasonication and 30 min centrifugation at 13,000×g. Supernatants were purified with 3 cm^3 60 mg Oasis HLB solid phase extraction columns. Growth medium was filtered with PVDF syringe filters prior to analysis.

O-Glucosyltransferase (O-GT, E.C. 2.4.1.x) was extracted based on the method described previously [26]. Three grams of hairy roots were homogenized and extracted with 100 mM sodium phosphate-buffer pH 6.5 containing 10 mM DTE, 2 mM MgCl$_2$, 1 mM EDTA, 1 mM PMSF and 1% PVP K90 at 4°C for 30 min. After centrifugation at 15,000×g for 30 min at 4°C, proteins in the supernatant were precipitated progressively by addition of ammonium sulphate to 40% and 75% saturation and centrifuged at 18,500×g for 30 min at 4°C, respectively. Consequently, the pellets were resuspended in 2.5 mL 200 mM Tris/HCl buffer with 2 mM MgCl$_2$ and 1 mM DTE, pH 7.3. Proteins were desalted by size exclusion chromatography through PD 10 columns (GE Healthcare, UK) and stored at −80°C before use.

2.5. LC-MS analysis

OBZ and metabolites were determined with a high-performance liquid chromatography (HPLC) system (Varian ProStar 210) coupled to an ion trap mass spectrometer (Varian 500-MS). A Phenomenex HYDRO-RP column (C18, polar endcapped; particle size 4 μm; 50 mm × 2.0 mm) was applied for separation of analytes using H$_2$O with 0.1% formic acid as mobile phase A, acetonitrile with 0.1% formic acid as mobile phase B with following gradient: 0–2 min 97% Buffer A; 2–10 min 95% Buffer B; 10–12 min 95% Buffer B; 12–12.5 min 97% Buffer A; 12.5–17 min 97% A. The flow rate was 0.3 mL/min. Concentration of OBZ was determined by an external standard calibration curve. The HPLC eluent was introduced into the mass spectrometer using a pneumatically assisted electro-spray source (positive mode). The interface was adjusted to the following conditions: capillary voltage, 63 V; needle voltage, 4,500 V; drying gas temperature, 300°C. MS/MS spectra were obtained by collision-induced dissociation using nitrogen as the collision gas.

2.6. Determination of O-GT activity

O-GT activity was determined using the method described by San Miguel et al. [26]. The reaction mixture contained 0.1 mM substrate (quercetin, kaempferol), 2 mM uridine 5′-diphophoglucose disodium salt, 3.125 mM 4-nitrophenyl β-d-glucuronide and 3.125 mM salicin in 200 mM Tris/HCl buffer (pH 7.3) with 2 mM MgCl$_2$. The reaction was started by adding 100 μL enzyme extract. After 30 min incubation at 30°C the reaction was stopped by protein precipitation with 10 μL concentrated phosphoric acid, after centrifugation at

15,000×g for 2 min. The supernatant was diluted 1:4 (v/v) with HPLC solvent A. Measurement was performed by the HPLC system (Varian Pro-Star M215) equipped with a C18 Prontosil Spheribond column (5 μM, 250 × 3.0 mm, Bischoff Chromatography, Leonberg). Mobile phases consist of 0.1% aqueous trifluoroacetic acid (TFA) as solvent A and acetonitrile with 0.1% TFA as solvent B. OBZ was separated with the following gradient: 0–8 min 92% B (isocratic); 8–9.5 min 100% B (linear increasing); 9.5–12.5 min 8% B (linear decreasing); 12.5–15 min 8% B (isocratic). The flow rate was kept at 0.85 mL/min and the analytes were detected via HPLC with UV detection at 370 nm (Varian ProStar 335, Germany). O-GT activity is expressed as the enzymatic formation of 1 pmol product per min [pkatal] in the enzyme extracts. Protein content was determined by the method of Bradford [27] with bovine serum albumin as a standard protein.

Kinetic analyses of the results obtained from directly adding 3 mg/L TiO$_2$ to the above described standard assays with various substrate concentrations (kaempferol, 0.06–0.14 μM) were performed using GraphPad Prism. Michaelis–Menten and Lineweaver–Burk plots were made to allow the calculation of Michaelis constant K_m values.

2.7. Data analysis

Statistical analyses were performed with the software GraphPad Prism v5.0. One-way analysis of variance (ANOVA) with Tukey posttest and two-way ANOVA with Bonferroni posttest were applied respectively to determine the significant differences between groups from seed germination tests and hairy roots experiment. Comparisons were considered significantly different for $p < 0.05$.

3. Results and discussion

3.1. Effect of OBZ and TiO$_2$ on plant growth

The potential effect of OBZ and TiO$_2$ on seed development was tested by calculating the germination rate and root length of tomato and barley. As shown in Fig. 1, treatment with OBZ and TiO$_2$ resulted in different germination patterns between tomato and barley. Addition of OBZ significantly inhibited germination rates of tomato seeds by 31.6%, accordingly, and the average root length of seeds germinated under OBZ treatment was 1.1 cm, which was 57.5% lower than that in the other treatments. Unlike studies which proposed the negative influence of nanoparticles on root length of tomato [28], this study did not detect effects of TiO$_2$ on seeds compared with nontreated seeds. However, TiO$_2$ reduced the impact of OBZ under the condition of simultaneous exposure, because the germination rate in the co-exposure was elevated and was similar to the control level, moreover, slightly longer root length (nonsignificant) was observed for seeds exposed to treatments containing TiO$_2$. This beneficial effect of TiO$_2$ has also been shown in *Arabidopsis thaliana* exposed to the antibiotic tetracycline, when the phytotoxicity of tetracycline on root elongation and biomass was alleviated in the presence of TiO$_2$. A possible explanation is that Ti nanoparticles interact with tetracycline outside of the plant, thus preventing the exposure at a micro-/nano-level; also, co-exposure increased
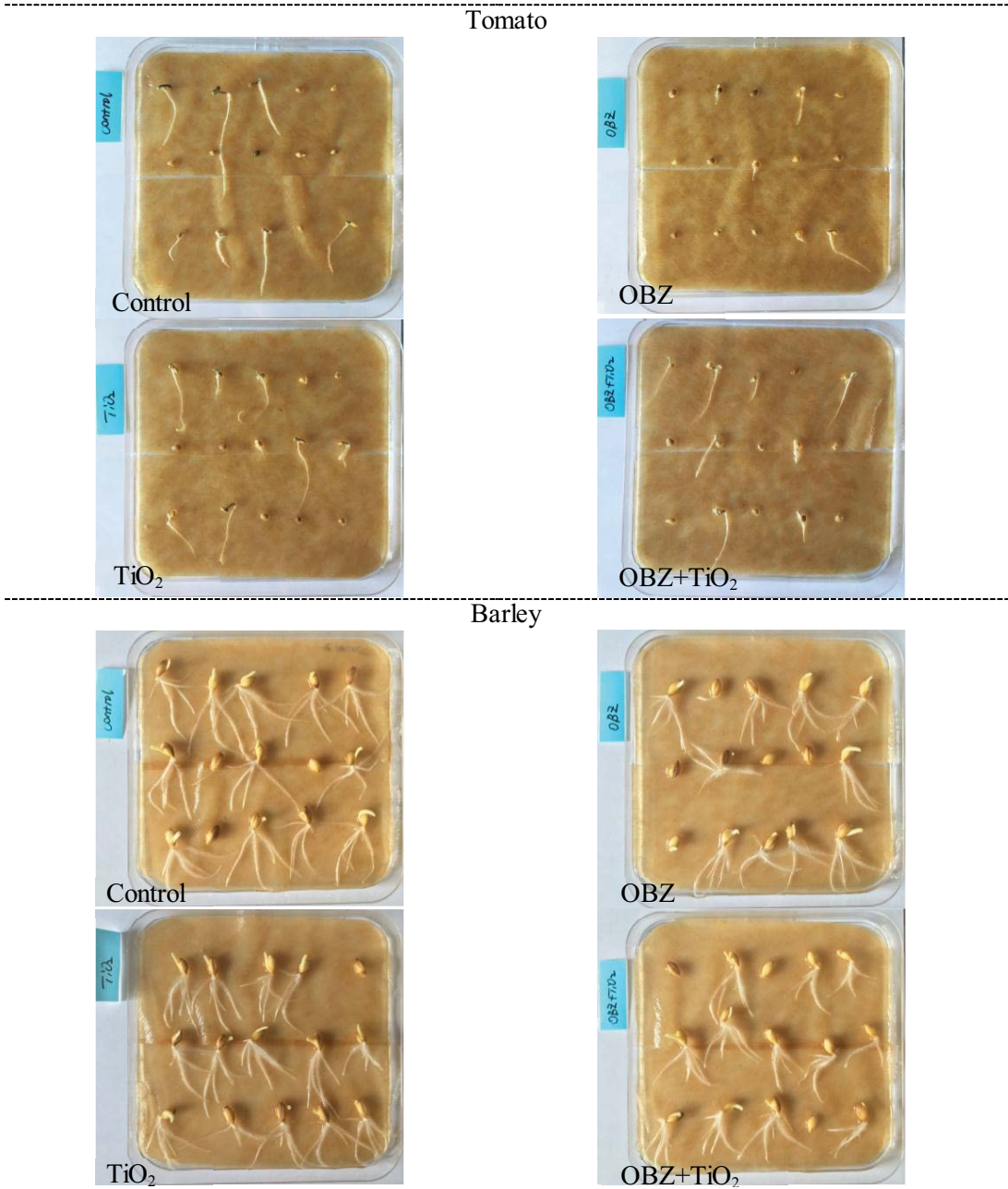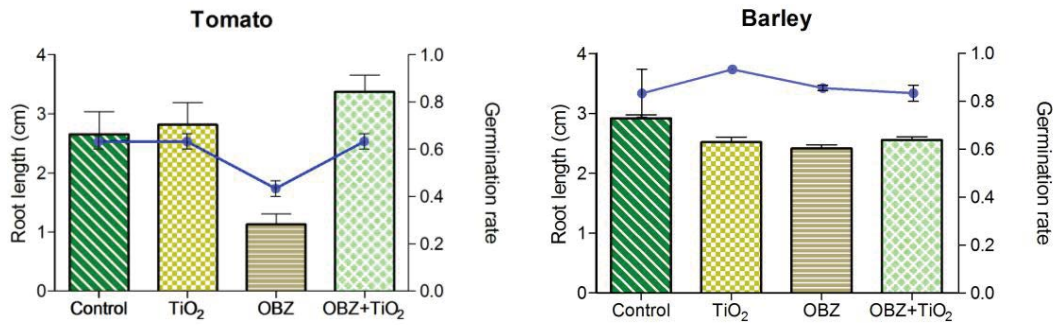
Fig. 1. Effects of 3 mg/L TiO_2 and 5 μM OBZ on the germination rate (line) and root length (column) of barley and tomato seedlings. Image of seeds exposed to different treatments. Seeds were germinated on wet filter paper for 3 and 10 d for barley and tomato, respectively. Error bars represent standard error of mean (n = 30).

plant total protein content, which plays an essential role in plant growth such as root elongation [29]. Similar to the present finding, Larue and coworkers [30] reported that TiO_2 in concentrations up to 100 mg/L did not pose impact on wheat and rapeseed germination rates, and induction of root elongation was found for both plant species upon exposure. Enhanced germination rate and growth was revealed in tomato grown in multiwall nanotube amended agar medium, presumably by affecting the expression of genes that facilitate cell division and development [31]. Another proposed mechanism is the facilitated water uptake due to the increasing number of surface defects on the seed coat by the nanoparticles [32]. In agreement with the statement of Begum and coworkers [28] the effects of nanoparticles differed among plant species. The test with barley seeds in this study shows no distinguished difference on the germination rate and root numbers (see Fig. 1) among all the treatments, however, compared with the seedlings in the control, the root length was significantly reduced by 15.2%–17.2% after addition of xenobiotics regardless of single or co-exposure treatment. The literature on the phytotoxicity of TiO_2 varies considerably with concentrations and plant species. Song and coworkers [33] showed that high concentrations of TiO_2 inhibited the growth of *L. minor*, on the other hand, frond numbers were stimulated at low concentrations.

The favourable effect of TiO_2 was again confirmed by a microbiotest with *Lemna* in this study. Regardless of single or co-exposure to TiO_2, the relative growth rate of fronds in these treatments was significantly higher (47%–49%) in comparison with the controls (Fig. 2). The results obtained from pigment measurements of corresponding fronds further support the aforementioned findings. Contents of chlorophylls (Chl) a and b were significantly lower in the plants exposed to OBZ compared with the controls, whereas addition of TiO_2 significantly increased Chl a, Chl b and carotenoids content by 42.2%, 63.8% and 46.5%, respectively, relative to the OBZ treatment alone (Fig. 3). Chlorophyll contents are important parameters to evaluate stress and toxicity to plants. Many studies have reported that TiO_2 could affect photosynthesis of plants, including variations on chlorophyll contents, photosynthetic rate and chloroplast structure. For example, the chlorophyll content was increased in *Lemna* or mung bean subjected to TiO_2 [33,34], and it was explained that TiO_2 might enter the chloroplast and its oxidation–reduction reactions might accelerate electron transport and oxygen evolution [33]. TiO_2 has also been shown to stabilize the integrity of chloroplast membranes and protect chloroplasts from aging [35]. Furthermore, net photosynthetic rate and Rubisco carboxylation were shown to be promoted under the treatment of TiO_2, resulting from the enhancement of activity of Rubisco through the increase of mRNA amounts and protein expression [36]. Although oxidative stress has been observed in plants exposed to TiO_2 [37], the better growth of plants under exposure to TiO_2 demonstrated that a certain amount of stress, which does not exceed the plant's anti-oxidative capacity, might be positive for plants. This is supported by the opinion of Mittler [38] that low level of reactive oxygen species (ROS) is beneficial, and is necessary for the activation of cellular proliferation, physiological function and viability. It was further speculated that in the case of dissociation of TiO_2, Ti^{4+} might
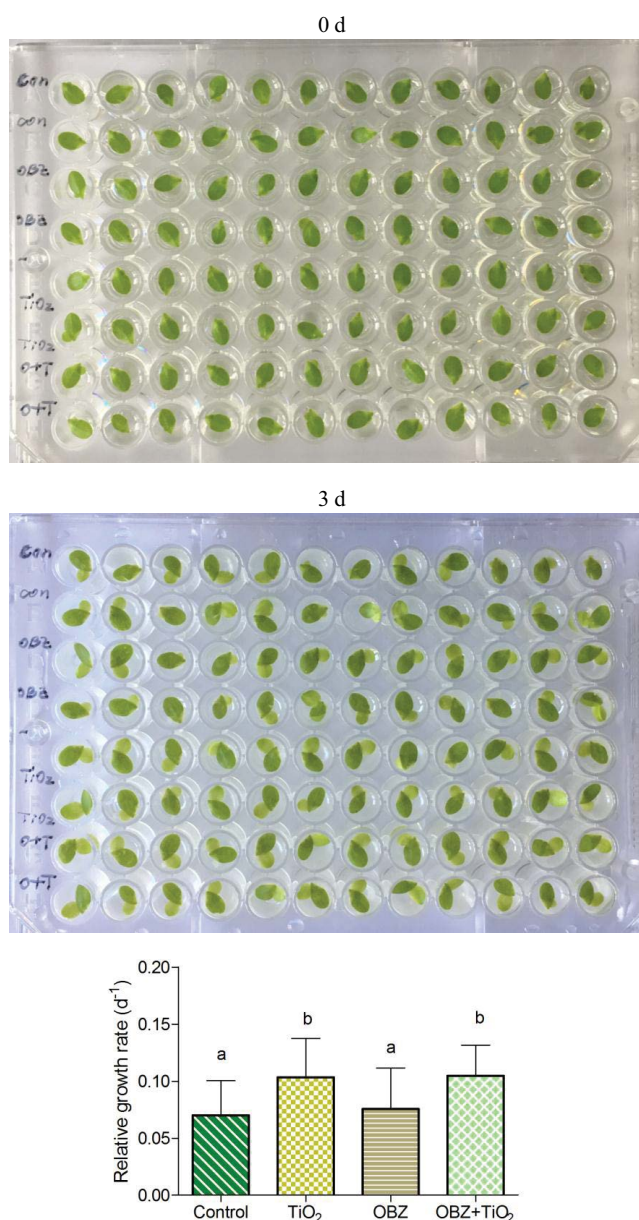

Fig. 2. Impact of 3 mg/L TiO_2 and 5 µM OBZ on the growth of *Lemna minor*. The relative growth rate (RGR) was quantified by measuring the frond area of *Lemna* before and after incubation for 3 d. RGR = (ln A_3 − ln A_0)/3, A_0 is the initial frond area (cm^2) at day 0 and A_3 is the area of corresponding frond at day 3. Error bars represent standard error of mean (*n* = 24). Lowercase letters indicate significant differences among different treatment groups according to ANOVA at $p < 0.05$.

transform the ROS O_2^- radicals which are damaging to the photosystem and may accelerate the aging [35].

3.2. Uptake of OBZ under co-exposure with TiO_2

During 1 week exposure to environmentally relevant concentrations of OBZ and TiO_2, OBZ was taken up continuously by roots regardless whether it was offered alone or together
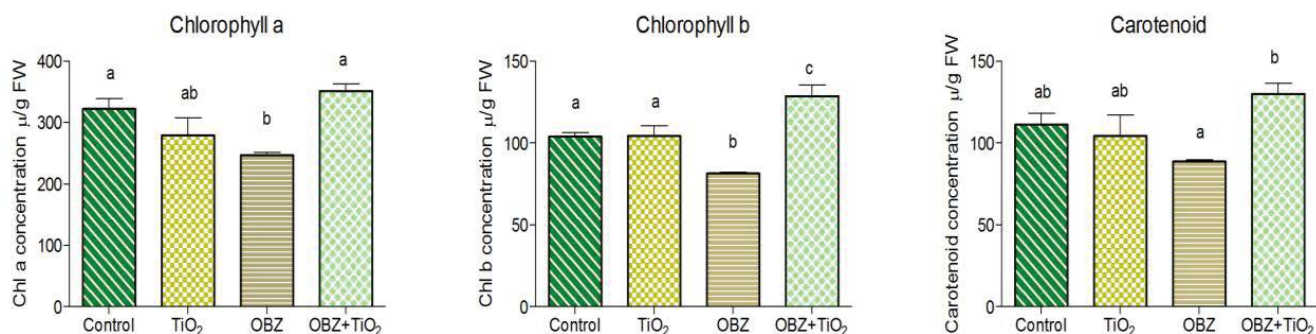
Fig. 3. Contents of photosynthetic pigments after 3-d exposure to different treatments. Values are mean of two replicates, each replicate contain fronds from 12 wells. Error bars indicate SD. Lowercase letters indicate significant differences among different treatment groups according to ANOVA at $p < 0.05$.

with TiO_2. As shown in Fig. 4, at the end of the experiment, uptake percentage reached 61.2% and 77.7% for OBZ alone and for TiO_2 co-exposure, respectively. Roots from controls and TiO_2 treatment alone were excluded from the figure as no OBZ was detected in those samples. Co-exposure to TiO_2 significantly ($p < 0.05$) increased accumulation of OBZ in roots. Compared with OBZ single exposure, the presence of TiO_2 enhanced OBZ amount in roots by 38% and 27% after 2 and 7 d incubation, respectively.

The majority of former studies had focused on the photodegradation of organic pollutants in the presence of TiO_2 as catalyst [39,40], while OBZ is not supposed to be photodegradable due to its property as sun-blocker [41]. Its photodynamics was proven to be stable in the co-existence of inorganic scatterer TiO_2, and very little interaction (adsorption) between the two species has been mentioned [42]. The results from medium free of roots confirmed the former findings, as shown in Fig. 5. Concentration of OBZ remained consistent except on day 7 when 27.6% of OBZ was lost under the condition of co-exposure. Few studies have been carried out to investigate the role of TiO_2 on the accumulation of organic pollutants by plants. Uptake of TiO_2 alone has been reported for several plant species, and TiO_2 particles with smaller diameters accumulated to a greater extent than the larger

ones [43]. In fact, plants may be able to increase the availability of TiO_2 by influencing the size of particles with root exudates, rhizosphere pH, etc. [17]. Nanoparticles of smaller size obtain new properties such as higher surface reactivity which might enlarge root pores or create new ones, leading to higher hydromineral flow and elevated nutrient uptake in roots [30], a process that might simultaneously increase the uptake of OBZ and explain the higher OBZ concentration observed during co-exposure with TiO_2. Previous results have shown that nanoparticles may induce the transport of secondary pollutants [30,42]. For example, uptake of arsenic (As) has been enhanced in the presence of graphene oxide (GO) nanomaterial via at least three pathways, including the enhanced permeability due to the structural damage to the cell wall, an up-regulation of transporter for As and the cotransport of As that had been absorbed on GO [44]. Additionally, in recent studies, interactions between phenanthrene and nanomaterial have been visualized, and multiwall carbon nanotubes have been shown to pierce wheat root cell walls and by that enhance the uptake of phenanthrene into the living cells [45].

3.3. Effect of TiO_2 on transformation of OBZ

After uptake, OBZ underwent metabolic transformation. Possible pathways of OBZ in HRs have been described
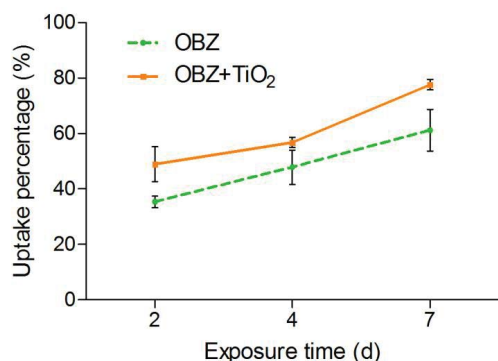

Fig. 4. Effect of TiO_2 on the uptake of OBZ into horseradish hairy roots, the uptake percentage of OBZ (%) = the mass of OBZ taken up by roots under exposure (µg)/the initial mass of OBZ in the hydroponic medium (µg), the mass of OBZ in roots = roots weight (g) × OBZ concentration in root (µg/g fresh weight (FW)). Error bars indicate SD ($n = 3$).
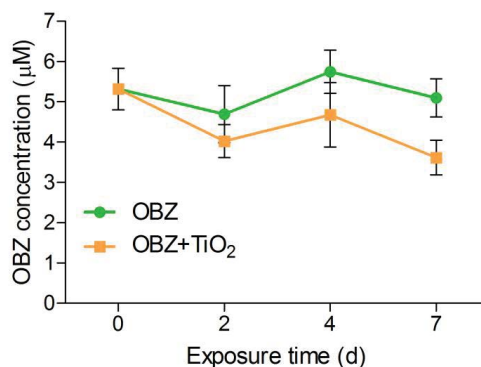

Fig. 5. OBZ concentration (µM) in medium without roots over incubation time. No statistical difference among exposure time (except day 7) according to ANOVA at $p < 0.05$. Error bars indicate standard deviation ($n = 3$).

previously [25], and current results confirmed the hypothesis that part of the accumulated OBZ would be transformed to yield an oxybenzone-glucoside (OBZ-Glu) and subsequently an oxybenzone-malonyl-glucoside (OBZ-Mal-Glu). Effects of TiO_2 on the transformation of OBZ were only recognized on the 4th day, when co-exposure with TiO_2 reduced the amount of OBZ-Glu to 76.5% of that in the OBZ alone condition (Fig. 6). The secondary transformation to OBZ-Mal-Glu was affected slightly by the addition of TiO_2, and a lower amount of OBZ-Mal-Glu was observed in the samples from co-exposure, while the difference was not statistically significant.

To further investigate the impact of TiO_2 on the detoxification mechanisms for OBZ, activity of *O*-glucosyltransferases (*O*-GT, E.C. 2.4.1.x) was assayed as they are representative enzymes participating in the phase II transformation of xenobiotics, including OBZ [46]. The involvement of the *O*-GT enzyme system is important in the responses of plant tissues to OBZ treatment, which have been confirmed

formerly to catalyse the glucosylation of OBZ to form OBZ-Glu [25]. Activity of *O*-GT was evaluated in standard assays with two natural substrates – quercetin and kaempferol. Consistent with previous findings showing that activities of *O*-GT were elevated to better transform the organic xenobiotic into a less toxic form [47,48], this study showed that after 4-d exposure in OBZ containing suspensions, *O*-GT$_{Quercetin}$ activities were stimulated significantly to 127.4% and 164.6%, and *O*-GT$_{Kaempferol}$ activities were enhanced to 118.3% and 131.2% of control for OBZ alone and co-exposure treatment, respectively (Fig. 7). Contrary to this stimulation, co-exposure with OBZ and TiO_2 showed 37.2% lower *O*-GT activity towards quercetin when compared to that level in the OBZ alone treatment. A similar pattern was also recorded for kaempferol as a substrate, where addition of TiO_2 to the OBZ treatment again lowered the *O*-GT activity, albeit the reduction was not statistically significant. The decrease of *O*-GT activity in enzyme extracts derived from the co-exposure experiments
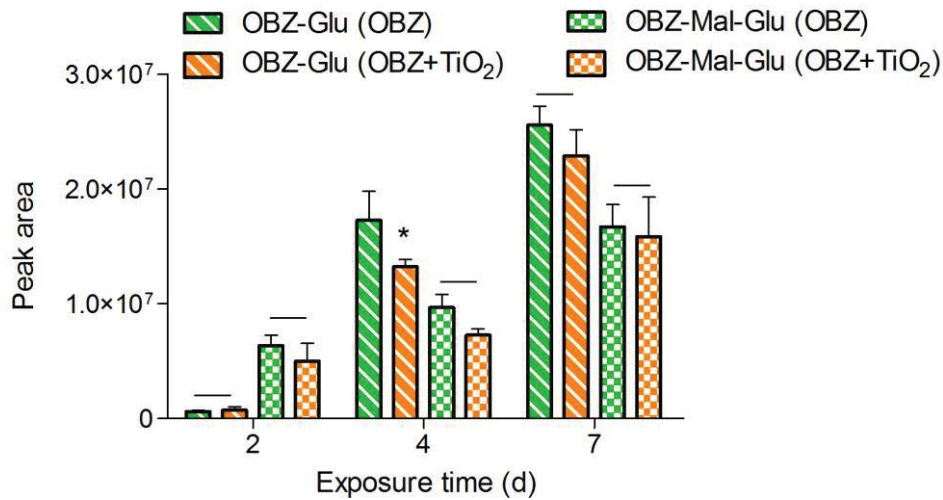

Fig. 6. Impact of TiO_2 on the formation of OBZ metabolites in horseradish hairy roots from OBZ single treatment (OBZ-Glu (OBZ), OBZ-Mal-Glu (OBZ)) and co-exposure treatment (OBZ-Glu (OBZ+TiO_2), OBZ-Mal-Glu (OBZ + TiO_2)) after 2, 4 and 7 d incubation. Values are mean of three parallel individuals, *$p < 0.05$.
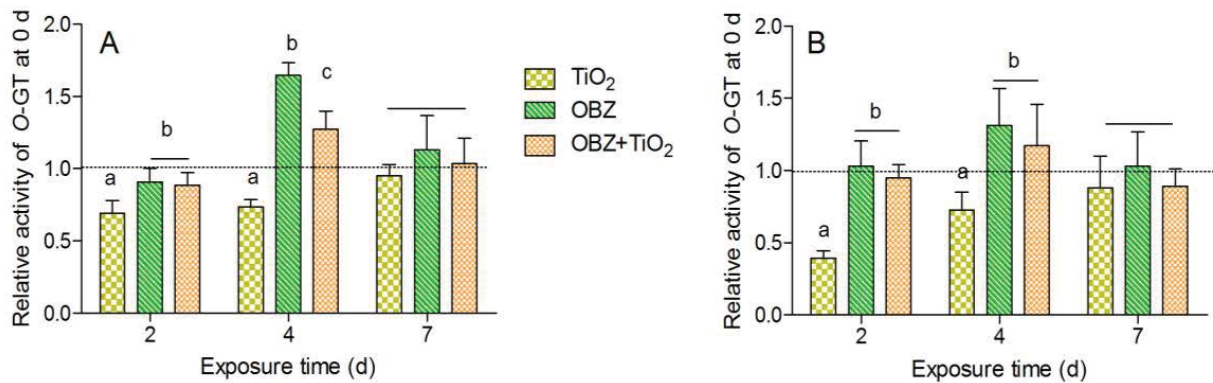

Fig. 7. Influences of OBZ and TiO_2 on the activities of *O*-GT in horseradish hairy roots collected from different treatments at each exposure time. *O*-GT activities (A: *O*-GT$_{Quercetin}$; B: *O*-GT$_{Kaempferol}$) are depicted relative to activities of root samples collected on the 0 d. Dashed lines are relative activities of control samples without OBZ and TiO_2. Error bars indicate SD ($n = 3$). Lowercase letters indicate significant differences among treatments according to ANOVA at $p < 0.05$.

corresponds to the lower amount of OBZ-Glu detected in the roots from the same treatment. This result implies that TiO_2 affected the transformation of OBZ in plant transiently, as after 7-d incubation, this negative effect was eliminated and the activity had recovered to the same level as that in controls. Inhibition of detoxification enzyme activities in the co-exposure to TiO_2 has also been reported by Liu and coworkers. They report that the addition of TiO_2 to *A. thaliana* exposed to tetracycline has reduced the activities of peroxidase and catalase [29]. In the present case, the inhibition effect was exaggerated when the hairy roots were treated with TiO_2 independently; the corresponding *O*-GT activity was suppressed significantly to 38%–69% of the activity in nontreated hairy root tissue. Similar inhibitory effects on the ability of plants to conjugate organic xenobiotics have also been found in plants subjected to heavy metals [49], and the same phenomenon has been demonstrated in vitro with isolated detoxification enzymes, which showed direct inhibition effect of cadmium on the catalytic reaction of glutathione reductase and glutathione-*S*-transferases [50]. The effect of TiO_2 on the *O*-GT activities was also investigated by in vitro incubation with TiO_2 directly added to the standard enzyme assays. As followed by Michaelis–Menten kinetics (Fig. S1), the K_m value for kaempferol with addition of TiO_2 ($K_m = 34.75 \pm 12.62$ µM) was not significantly higher than that determined for kaempferol alone ($K_m = 23.17 \pm 6.25$ µM). This indicates that TiO_2 had no significant influence on catalytic properties of the *O*-GT involved.

4. Conclusion

The findings in this study show that addition of TiO_2 may reduce the negative impact of OBZ, since elevated germination rate and root length were observed in the co-exposure situation. Moreover, the highest growth rate and pigment contents were detected in *Lemna* grown under the influence of both substances. Paradoxically, plants used for remediating OBZ can eventually be expected to encounter lower toxicity when co-exposed to TiO_2. The HRs is an efficient model to study plant short-term response with respect to OBZ and TiO_2. The results show that OBZ loaded with TiO_2 may increase the bioaccumulation of OBZ in plant, because more OBZ was incorporated into roots with the presence of TiO_2 in the hydroponic system. Activity of *O*-GT was elevated to detoxify the xenobiotic OBZ, and OBZ was continuously transformed to OBZ-malonyl-glucoside.

The present research complements the former results about the removal of single contaminant OBZ, as it aids in understanding the influence of co-occurring nanoparticles on the plant remediation process of OBZ. The potential of phytoremediation must be scrutinized by considering detailed field studies with mixed pollution, to better forecast the performance of plants under the influence of real-world scenarios.

Acknowledgements

References

[1] K. Fent, A. Zenker, M. Rapp, Widespread occurrence of estrogenic UV-filters in aquatic ecosystems in Switzerland, Environ. Pollut., 158 (2010) 1817–1824.
[2] N. Serpone, D. Dondi, A. Albini, Inorganic and organic UV filters: their role and efficacy in sunscreens and suncare products, Inorg. Chim. Acta, 360 (2007) 794–802.
[3] C. Liao, K. Kannan, Widespread occurrence of benzophenone-type UV light filters in personal care products from China and the United States: an assessment of human exposure, Environ. Sci. Technol., 48 (2014) 4103–4109.
[4] M.M.P. Tsui, H.W. Leung, B.K.Y. Kwan, K.Y. Ng, N. Yamashita, S. Taniyasu, P.K.S. Lam, M.B. Murphy, Occurrence, distribution and ecological risk assessment of multiple classes of UV filters in marine sediments in Hong Kong and Japan, J. Hazard. Mater., 292 (2015) 180–187.
[5] W. Li, Y. Ma, C. Guo, W. Hu, K. Liu, Y. Wang, T. Zhu, Occurrence and behavior of four of the most used sunscreen UV filters in a wastewater reclamation plant, Water Res., 41 (2007) 3506–3512.
[6] A. Sánchez Rodríguez, M. Rodrigo Sanz, J.R. Betancort Rodríguez, Occurrence of eight UV filters in beaches of Gran Canaria (Canary Islands). An approach to environmental risk assessment, Chemosphere, 131 (2015) 85–90.
[7] M.E. Balmer, H.R. Buser, M.D. Müller, T. Poiger, Occurrence of some organic UV filters in wastewater, in surface waters, and in fish from Swiss lakes, Environ. Sci. Technol., 39 (2005) 953–962.
[8] C.A. Downs, E. Kramarsky-Winter, R. Segal, J. Fauth, S. Knutson, O. Bronstein, F.R. Ciner, R. Jeger, Y. Lichtenfeld, C.M. Woodley, P. Pennington, K. Cadenas, A. Kushmaro, Y. Loya, Toxicopathological effects of the sunscreen UV filter, Oxybenzone (Benzophenone-3), on coral planulae and cultured primary cells and its environmental contamination in Hawaii and the U.S. Virgin islands, Arch. Environ. Contam. Toxicol., 70 (2016) 265–288.
[9] N. Blüthgen, S. Zucchi, K. Fent, Effects of the UV filter benzophenone-3 (oxybenzone) at low concentrations in zebrafish (*Danio rerio*), Toxicol. Appl. Pharmacol., 263 (2012) 184–194.
[10] R. Danovaro, L. Bongiorni, C. Corinaldesi, D. Giovannelli, E. Damiani, P. Astolfi, L. Greci, A. Pusceddu, Sunscreens cause coral bleaching by promoting viral infections, Environ. Health Perspect., 116 (2008) 441–447.
[11] C.O. Robichaud, A.E. Uyar, M.R. Darby, L.G. Zucker, M.R. Wiesner, Estimates of upper bounds and trends in nano-TiO_2 production as a basis for exposure assessment, Environ. Sci. Technol., 43 (2009) 4227–4233.
[12] M.A. Kiser, P. Westerhoff, T. Benn, Y. Wang, J. Pérez-Rivera, K. Hristovski, Titanium nanomaterial removal and release from wastewater treatment plants, Environ. Sci. Technol., 43 (2009) 6757–6763.
[13] F. Chen, C. Huber, P. Schröder, Fate of the sunscreen compound Oxybenzone in *Cyperus alternifolius* based hydroponic culture: uptake, biotransformation and phytotoxicity, Chemosphere, 182 (2017) 638–646.
[14] M.F. Serag, N. Kaji, C. Gaillard, Y. Okamoto, K. Terasaka, M. Jabasini, M. Tokeshi, H. Mizukami, A. Bianco, Y. Baba, Trafficking and subcellular localization of multiwalled carbon nanotubes in plant cells, ACS Nano, 5 (2011) 493–499.
[15] R. De La Torre-Roche, J. Hawthorne, Y. Deng, B. Xing, W. Cai, L.A. Newman, Q. Wang, X. Ma, H. Hamdi, J.C. White, Multiwalled carbon nanotubes and C_{60} fullerenes differentially impact the accumulation of weathered pesticides in four agricultural plants, Environ. Sci. Technol., 47 (2013) 12539–12547.
[16] X. Zhang, H. Sun, Z. Zhang, Q. Niu, Y. Chen, J.C. Crittenden, Enhanced bioaccumulation of cadmium in carp in the presence of titanium dioxide nanoparticles, Chemosphere, 67 (2007) 160–166.
[17] D.L. Jacob, J.D. Borchardt, L. Navaratnam, M.L. Otte, A.N. Bezbaruah, Uptake and translocation of Ti from nanoparticles in crops and wetland plants, Int. J. Phytorem., 15 (2013) 142–153.
[18] K. Ganguly, S. Upadhyay, M. Irmler, S. Takenaka, K. Pukelsheim, J. Beckers, E. Hamelmann, H. Schulz, T. Stoeger, Pathway

focused protein profiling indicates differential function for IL-1B, -18 and VEGF during initiation and resolution of lung inflammation evoked by carbon nanoparticle exposure in mice., Part. Fibre Toxicol., 6 (2009) 31.

[19] A. Stampfl, M. Maier, R. Radykewicz, P. Reitmeir, M. Göttlicher, R. Niessner, Langendorff heart: a model system to study cardiovascular effects of engineered nanoparticles, ACS Nano, 5 (2011) 5345–5353.

[20] *Spirodela* duckweed toxkit a simple and practical growth inhibition microbiotest with *Spirodela polyrhiza* bench protocol, Available at: http://www.ebpi-kits.com/images/spirodelastp. pdf (accessed October 4, 2017).

[21] OECD, Test No. 221: *Lemna* spp. Growth Inhibition Test, OECD Guidel. Test. Chem. Sect. 2. OECD Publishing, Paris, 2006, pp. 1–22.

[22] M. Obermeier, C.A. Schröder, B. Helmreich, P. Schröder, The enzymatic and antioxidative stress response of *Lemna minor* to copper and a chloroacetamide herbicide, Environ. Sci. Pollut. Res., 22 (2015) 18495–18507.

[23] H.K. Lichtenthaler, C. Buschmann, Chlorophylls and carotenoids: measurement and characterization by UV-VIS spectroscopy, Curr. Protoc. Food Anal. Chem., 1 (2001) F4.3.1-F4.3.8.

[24] A. Nepovím, R. Podlipná, P. Soudek, P. Schröder, T. Vaněk, Effects of heavy metals and nitroaromatic compounds on horseradish glutathione S-transferase and peroxidase, Chemosphere, 57 (2004) 1007–1015.

[25] F. Chen, C. Huber, R. May, P. Schröder, Metabolism of Oxybenzone in a hairy root culture: perspectives for phytoremediation of a widely used sunscreen agent, J. Hazard. Mater., 306 (2016) 230–236.

[26] A. San Miguel, P. Schröder, R. Harpaintner, T. Gaude, P. Ravanel, M. Raveton, Response of phase II detoxification enzymes in *Phragmites australis* plants exposed to organochlorines, Environ. Sci. Pollut. Res., 20 (2013) 3464–3471.

[27] M.M. Bradford, A rapid and sensitive method for the quantitation of microgram quantities of protein utilizing the principle of protein-dye binding, Anal. Biochem., 72 (1976) 248–254.

[28] P. Begum, R. Ikhtiari, B. Fugetsu, Graphene phytotoxicity in the seedling stage of cabbage, tomato, red spinach, and lettuce, Carbon N. Y., 49 (2011) 3907–3919.

[29] H. Liu, C. Ma, G. Chen, J.C. White, Z. Wang, B. Xing, O.P. Dhankher, Titanium dioxide nanoparticles alleviate tetracycline toxicity to *Arabidopsis thaliana* (L.), ACS Sustainable Chem. Eng., 5 (2017) 3204–3213.

[30] C. Larue, G. Veronesi, A.-M. Flank, S. Surble, N. Herlin-Boime, M. Carrière, Comparative uptake and impact of TiO_2 nanoparticles in wheat and rapeseed, J. Toxicol. Environ. Health Part A, 75 (2012) 722–734.

[31] M.V. Khodakovskaya, B.-S. Kim, J.N. Kim, M. Alimohammadi, E. Dervishi, T. Mustafa, C.E. Cernigla, Carbon nanotubes as plant growth regulators: effects on tomato growth, reproductive system, and soil microbial community, Small, 9 (2013) 115–123.

[32] M. Vithanage, M. Seneviratne, M. Ahmad, B. Sarkar, Y.S. Ok, Contrasting effects of engineered carbon nanotubes on plants: a review, Environ. Geochem. Health, 39 (2017) 1421–1439.

[33] G. Song, Y. Gao, H. Wu, W. Hou, C. Zhang, H. Ma, Physiological effect of anatase TiO_2 nanoparticles on *Lemna minor*, Environ. Toxicol. Chem., 31 (2012) 2147–2152.

[34] R. Raliya, P. Biswas, J.C. Tarafdar, TiO_2 nanoparticle biosynthesis and its physiological effect on mung bean (*Vigna radiata* L.), Biotechnol. Rep. (Amst.), 5 (2015) 22–26.

[35] F. Hong, F. Yang, C. Liu, Q. Gao, Z. Wan, F. Gu, C. Wu, Z. Ma, J. Zhou, P. Yang, Influences of nano-TiO_2 on the chloroplast aging of spinach under light., Biol. Trace Elem. Res., 104 (2005) 249–60.

[36] X. Wang, F. Gao, L. Ma, J. Liu, S. Yin, P. Yang, F. Hong, Effects of nano-anatase on ribulose-1, 5-bisphosphate carboxylase/oxygenase mRNA expression in spinach, Biol. Trace Elem. Res., 126 (2008) 280–289.

[37] A. Spengler, L. Wanninger, S. Pflugmacher, Oxidative stress mediated toxicity of TiO_2 nanoparticles after a concentration and time dependent exposure of the aquatic macrophyte *Hydrilla verticillata*, Aquat. Toxicol., 190 (2017) 32–39.

[38] R. Mittler, ROS are good, Trends Plant Sci., 22 (2017) 11–19.

[39] J. Zhao, C. Chen, W. Ma, Photocatalytic degradation of organic pollutants under visible light irradiation, Top. Catal., 35 (2005) 269–278.

[40] E. Pelizzetti, C. Minero, Mechanism of the photo-oxidative degradation of organic pollutants over TiO_2 particles, Electrochim. Acta, 38 (1993) 47–55.

[41] Y.S. Liu, G.G. Ying, A. Shareef, R.S. Kookana, Photostability of the UV filter benzophenone-3 and its effect on the photodegradation of benzotriazole in water, Environ. Chem., 8 (2011) 581–588.

[42] L.A. Baker, L.C. Grosvenor, M.N.R. Ashfold, V.G. Stavros, Ultrafast photophysical studies of a multicomponent sunscreen: oxybenzone–titanium dioxide mixtures, Chem. Phys. Lett., 664 (2016) 39–43.

[43] C. Larue, J. Laurette, N. Herlin-Boime, H. Khodja, B. Fayard, A.-M. Flank, F. Brisset, M. Carriere, Accumulation, translocation and impact of TiO_2 nanoparticles in wheat (*Triticum aestivum* spp.): influence of diameter and crystal phase, Sci. Total Environ., 431 (2012) 197–208.

[44] X. Hu, J. Kang, K. Lu, R. Zhou, L. Mu, Q. Zhou, Graphene oxide amplifies the phytotoxicity of arsenic in wheat, Sci. Rep., 4 (2015) 6122.

[45] E. Wild, K.C. Jones, Novel method for the direct visualization of in vivo nanomaterials and chemical interactions in plants, Environ. Sci. Technol., 43 (2009) 5290–5294.

[46] H. Sandermann, Plant metabolism of xenobiotics, Trends Biochem. Sci., 17 (1992) 82–84.

[47] M. Brazier, D.J. Cole, R. Edwards, O-glucosyltransferase activities toward phenolic natural products and xenobiotics in wheat and herbicide-resistant and herbicide-susceptible black-grass (*Alopecurus myosuroides*), Phytochemistry, 59 (2002) 149–156.

[48] B. Messner, O. Thulke, A.R. Schäffner, *Arabidopsis* glucosyltransferases with activities toward both endogenous and xenobiotic substrates, Planta, 217 (2003) 138–46.

[49] P. Schröder, L. Lyubenova, C. Huber, Do heavy metals and metalloids influence the detoxification of organic xenobiotics in plants?, Environ. Sci. Pollut. Res., 16 (2009) 795–804.

[50] L. Lyubenova, C. Götz, A. Golan-Goldhirsh, P. Schröder, Direct effect of Cd on glutathione S-transferase and glutathione reductase from *Calystegia sepium*, Int. J. Phytorem., 9 (2007) 465–473.

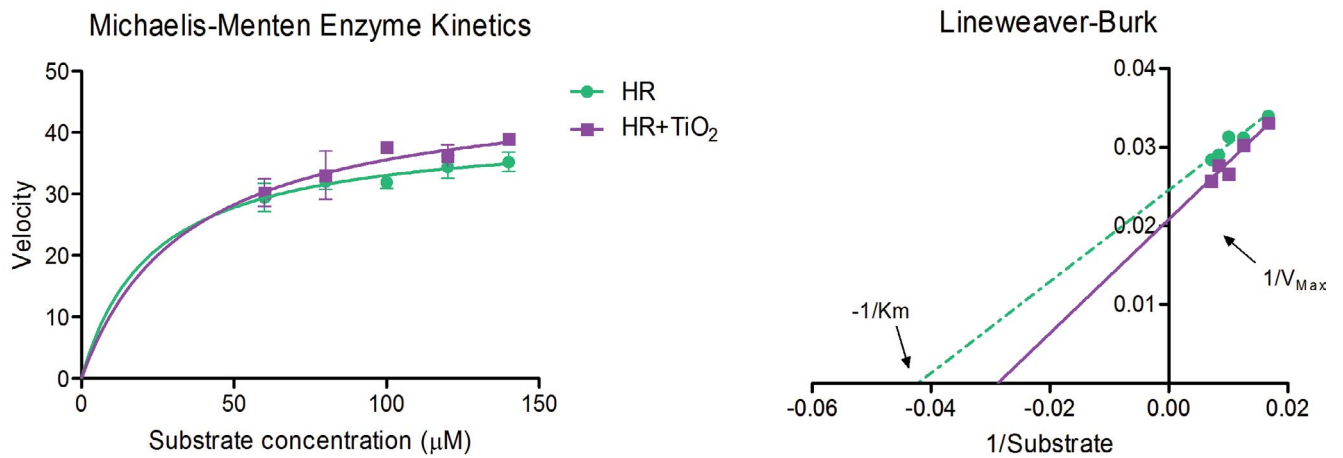**Supplementary information:**

Fig. S1. Response of *O*-GT activity to increasing substrate (kaempferol) concentrations. Filled circles and squares present the mean of three independent measurements. The best fit using Michaelis–Menten enzyme kinetics is displayed on the left side, and the corresponding Lineweaver–Burk plots for *O*-GT are presented on the right side. HR: assay with O-GT extracted from control hairy roots without any treatments; HR + TiO$_2$: *O*-GT assay in the presence of TiO$_2$. Note that during the preparation of the assay, precipitation of the substrate was observed under the influence of TiO$_2$. Despite this, the initial catalytic capacities are similar between two groups (HR + TiO$_2$; HR).